ELSEVIER

Catalysis Today 54 (1999) 245–253

CATALYSIS TODAY

www.elsevier.com/locate/cattod

Photocatalytic oxidation of cyanide in aqueous TiO_2 suspensions irradiated by sunlight in mild and strong oxidant conditions

V. Augugliaro [a,*], J. Blanco Gálvez [b], J. Cáceres Vázquez [b], E. García López [a], V. Loddo [a], M.J. López Muñoz [c], S. Malato Rodríguez [b], G. Marcì [a], L. Palmisano [a], M. Schiavello [a], J. Soria Ruiz [c]

[a] *Dipartimento di Ingegneria Chimica dei Processi e dei Materiali, Università di Palermo, Viale delle Scienze, 90128 Palermo, Italy*
[b] *Plataforma Solar de Almería, P.O. Box 22, 04200 Tabernas (Almeria), Spain*
[c] *Instituto de Catálisis y Petroleoquímica, CSIC, Campus de la Universidad Autónoma, Cantoblanco, 28049 Madrid, Spain*

Abstract

The photocatalytic oxidation of free cyanide ions was carried out in aqueous aerated suspensions containing polycrystalline TiO_2 (anatase) irradiated by sunlight. The influence of the presence of an organic compound (phenol) or of a strong oxidant (H_2O_2) on the photoprocess was also studied. The dependence of cyanide photo-oxidation rate on the following parameters: (1) cyanide concentration; (2) catalyst amount; and (3) phenol concentration was investigated. At the used experimental conditions, the kinetics of cyanide photo-oxidation is independent of the initial cyanide concentration and of the catalyst amount while it is affected by the phenol concentration and by the presence of H_2O_2. The Langmuir–Hinshelwood kinetic model has been used for phenomenologically describing the photoreactivity results. The reaction pathway was also investigated: cyanate, nitrite, nitrate and carbonate were found to be the main oxidation products. The mass balance of nitrogen was achieved only in strongly oxidant conditions; this insight suggests that some volatile nitrogen-containing species are formed at mild oxidation conditions.

Keywords: Photocatalysis; Cyanide photo-oxidation; Sunlight use; TiO_2 catalyst

1. Introduction

In the last years, photocatalysis by polycrystalline semiconductors irradiated by near-UV light has been found effective in oxidising certain organic and inorganic pollutants to less dangerous species in mild reaction conditions [1,2]. This method showed to be suitable for the oxidation of free and complex cyanides dissolved in water [3–7]. Free cyanide species are generated in large quantities in heat-treating operations and in the metal-finishing industry [8,9]. The greatest amounts of cyanide-containing wastes are produced by precious metals milling operations and coal gasification processes. The conventional processes used to treat waste waters polluted with cyanides are mainly chemical [10] and biological [11]. These methods present some drawbacks; for instance, in the alkaline chlorination process the formation of highly toxic cyanogen chloride gas can occur, while for biologic processes, even when the difficult problem of activated sludge disposal is overcome, the reaction rate values can be very low. Although the literature reports exhaustive studies [3–7], on the kinetic and mechanistic aspects of cyanides photo-oxidation carried out

* Corresponding author.

0920-5861/99/$ – see front matter
PII: S0920-5861(99)00186-8

in laboratory photoreactors using different lamps as radiation source, it seems useful to investigate the possibility of carrying out this photoreaction using sunlight as radiation source. The use of solar energy to remove CN^- ions is of great interest as it would drastically reduce the operational costs of a treatment process based on heterogeneous photocatalysis.

In the recent past, various kinds of solar photoreactors [12–14] have been used for performing the detoxification of water containing dangerous organic compounds. These investigations were focused on the obtaining information useful for the application of the photocatalytic method to environmental remediation.

On this background, the present paper is devoted to studying the photocatalytic oxidation of free cyanides by using polycrystalline TiO_2 (P25 Degussa) in a low-concentration solar radiation photoreactor. The influence on the photoprocess of mild or strong oxidation conditions of the reacting solution was investigated in the following conditions:

1. by saturating the dispersion with air at atmospheric pressure; or
2. by adding H_2O_2 to the dispersion in large excess with respect to the oxidisable species.

In real waste waters, the cyanide contamination is generally accompanied by the presence of several organic compounds. This fact determines that the efficiency of cyanide oxidation process may be lowered by the occurrence of competitive oxidation reactions regarding the organic compounds present in the solution. In order to have information on the competition process, the cyanide photoreactivity has also been studied by adding to the cyanide solution different amounts of phenol that is an organic contaminant typical of industrial waste waters. The kinetics of the photo-oxidation reaction has been investigated by varying the initial cyanide concentration and the molar ratio between the initial concentrations of cyanide ion and phenol. An investigation of the main intermediates was also carried out in order to hypothesise a likely reaction mechanism.

2. Experimental

The photoreactivity experiments were carried out using compound parabolic collectors (CPC) (Industrial Solar Technology, Denver), installed at the 'Plataforma Solar of Almería' (PSA). The photoreactor configuration, reported in Fig. 1, was a commonly used one in heterogeneous photocatalysis: a plug-flow photoreactor (PFP) in a recirculation loop with a well-stirred non-reacting tank (SNT) whose function was that of providing aeration and samples for analyses. The photoreactor consisted of six CPC modules in series (total reflective surface: 8.9 m^2) placed on fixed supports inclined at 37° (latitude of the PSA) with respect to the horizontal plane and facing South, in order to maximise the performance. Each CPC module consisted of eight parallel CPC reflectors (1.22 m long and 152 mm wide) with reflective surface made by polished aluminium. The plug-flow reactor comprised UV-transparent fluoropolymer tubes (i.d. 48 mm). All the tubes, as also the collectors, were connected in series and the aqueous dispersion was continuously fed from a reservoir tank by means of a centrifugal pump. The flow rate of the dispersion was maintained constant for all the runs; its value was ca. 1 dm^3/s corresponding to a Reynolds number of about 2.6×10^4 so that the flow regime inside the tubes was completely turbulent. The total volume of solution, V_T, which was charged in the photoreacting system, was 247 dm^3. The PFP volume, V_{PFP}, calculated as the volume of all the irradiated fluoropolymer tubes, was 108 dm^3. The mean residence time of the dispersion inside the PFP was 108 s. The catalyst used for the photoreactivity experiments was polycrystalline TiO_2 (P25, Degussa, ca. 80% anatase and 20% rutile, BET surface area of ca. 50 m^2/g).

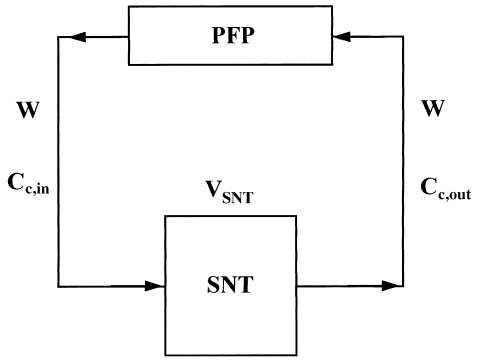

Fig. 1. Scheme of the photoreacting system. PFP, plug flow photoreactor; SNT, stirred non-reacting tank; *W*, liquid flow rate; $C_{c,in}$ and $C_{c,out}$, cyanide concentrations at inlet and outlet of SNT.

The experimental runs were carried out in the August–September period by using the following procedure. The reacting mixture was prepared in the stirred tank by firstly adding NaOH to distilled water to adjust the pH to 10; then the required amounts of NaCN and catalyst were added. The suspension was, therefore, fed to the tubes while maintaining the collectors covered. After 20 min of operation, corresponding to about five total residence times, the cover was removed and samples of the suspension at the exit of the SNT were withdrawn at fixed intervals of time. Some runs were carried out using cyanate as the starting reagent and by adding hydrogen peroxide to the system during the occurrence of the photoreaction. The $H_2O_2 : CNO^-$ molar ratio was chosen equal to 4 : 1 on the basis that the complete oxidation of a mole of CNO^- to CO_2 and $NO_3{}^-$ needs four moles of H_2O_2. The quantitative determination of cyanide was routinely performed by an ion-sensitive cyanide electrode (ORION mod. 94-06) in an expandable ion analyser (ORION 520 A). The oxygen needed for the photoreaction was derived from the contact of the suspension with the atmospheric air in the stirred tank. The cyanide initial concentration ranged between 0.19 and 2.4 mM; the catalyst amounts were in the 0.1–0.5 g/l range.

Some photoreactivity runs lasted for a very long time in order to determine the intermediates and final products of cyanide photo-oxidation. These experiments indicated that cyanate, nitrite, nitrate and carbonate were the main products. The quantitative determination of these anions was carried out by using an ionic chromatograph system (Dionex DX 120) equipped with an Ion Pac column (250 mm long). Aqueous solutions of $NaHCO_3$ (1 mM) and Na_2CO_3 (3.5 mM) were used as eluents at the flow rate of 1.67×10^{-2} cm^3/s.

In order to test the influence of aromatic species on the cyanide photo-oxidation rate, three runs were carried out by adding phenol as a model compound. For these runs, the initial cyanide and phenol concentrations, expressed in mM, were: (0.38, 0.38), (1.92, 0.38) and (1.92, 0.077), respectively; in this way, the molar ratios between initial cyanide and phenol were 1, 5, and 25, respectively. Two runs, at equal reaction conditions as compared to the previous ones, were also carried out by adding only phenol to the suspension; the initial phenol concentrations were 0.38 and 0.077 mM, respectively. The phenol analysis was performed by using a HPLC (Hewlett–Packard 1050) equipped with a C18 column (125 mm long). An aqueous solution of methanol (60% volume) was used as eluent at the flow rate of 1.67×10^{-2} cm^3/s. Total organic carbon (TOC) determinations were performed with a TOC analyser (Heraeus–Foss Electric TOC-2001).

In order to compare experimental runs carried out with different solar irradiances, the values of irradiance were monitored and recorded during the runs by using a sensor for global UV-light measurements (Eppley-TUVR) installed in the same position of the CPCs.

Some runs were carried out on bench scale by using a 500-ml laboratory batch photoreactor with an immersed lamp. A 125-W medium pressure Hg lamp was used for irradiating aqueous. aerated suspensions containing a catalyst amount of 0.2 g/l. This system simulated the mild oxidant conditions of the PFP. These runs, devoted to investigate the cyanide photodegradation mechanism, were carried out by using CNO^- or NH_2OH as substrates in order to check the presence, if any, of NH_3, $NO_2{}^-$ and $NO_3{}^-$. The initial cyanate and hydroxylamine concentrations were 1.2 mM. In these runs only qualitative analytical tests [15] were used. The direct Nesslerization method revealed the precipitation of Hg introduced as HgI_2 by the reducing species NH_2OH and the presence of NH_3 from the yellow coloration of the solution. The brucine method with, and without, the addition of sulphanilic acid, was used to check the presence of nitrate and/or nitrite ions, respectively.

3. Results

Preliminary photoreactivity runs were carried out at equal reaction conditions, but at different catalyst amounts, in the 0.1–0.5 g/l range. The obtained results did not differ appreciably among them so that the successive runs were performed with a constant catalyst amount of 0.2 g/l.

In order to compare the photoreactivity results obtained under different conditions of irradiation, the measured values of cyanide concentration have been considered as a function not of the reaction time but of the cumulative photonic energy, $E_{h\nu}$, incident on the reactor [12]. This quantity is given by:

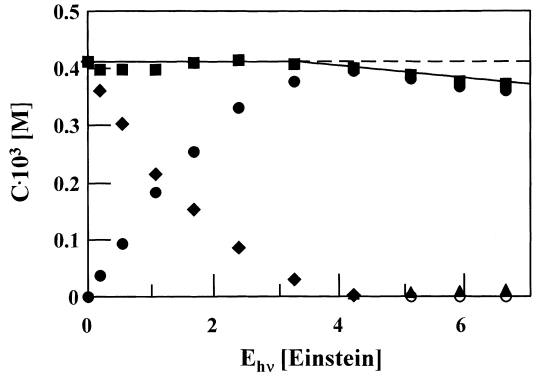

Fig. 2. Concentrations of cyanide (◆), cyanate (●), nitrite (▲), nitrate (○), and nitrogen balance (■) vs. the cumulative photonic energy, $E_{h\nu}$. Initial cyanide concentration: 0.41 mM.

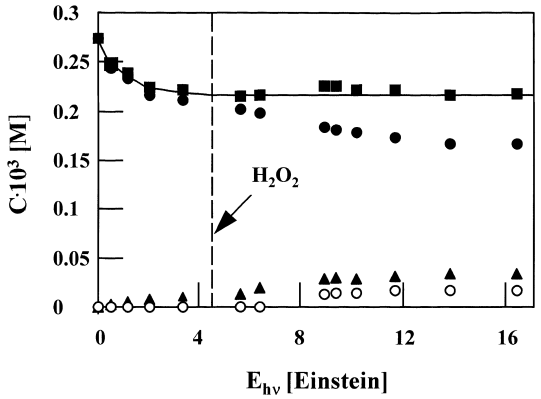

Fig. 3. Concentrations of cyanate (●), nitrite (▲), nitrate (○), and nitrogen balance (■) vs. cumulative photonic energy, $E_{h\nu}$,. Initial cyanate concentration: 0.27 mM.

$$E_{h\nu} = It \tag{1}$$

where I is the photon flow [Einstein/s] and t the irradiation time. The values of I were calculated from the irradiance data, by using the following relationship:

$$I = UV_G S \tag{2}$$

where S is the geometrical irradiated surface and UV_G the irradiance expressed as W/m^2. The UV_G dimensions were transformed in [Einstein/s m^2] by using the Planck's equation ($E = hc/\lambda$). By considering that the TiO_2 (anatase) band-gap energy corresponds to a wavelength of 387 nm, the conversion factor between [W/m^2] and [Einstein/s m^2] has the value of 3.23×10^{-6}.

Degradation runs carried out at different irradiance values did not show appreciable differences when the cyanide concentration results were plotted against the corresponding $E_{h\nu}$ figures. This finding indicates that the $E_{h\nu}$ quantity is the correct one for comparing reactivity results obtained at different radiation intensities owing to the fact that, in the used experimental conditions, the cyanide photodegradation rate depends linearly on the radiation intensity.

For a typical run carried out with a catalyst amount of 0.2 g/l, Fig. 2 reports the experimental values of cyanide, cyanate, nitrite and nitrate concentrations versus $E_{h\nu}$. In Fig. 2, the nitrogen mass balance is also reported. It can be observed that the balance is satisfied during the course of cyanide photo-oxidation, but it is not satisfied during the subsequent cyanate photo-oxidation. In order to better understand this behaviour, which was shown by all the runs, some runs were carried out using cyanate as the starting reagent and by adding hydrogen peroxide to the system during the occurrence of the photoreaction. For a representative run, Fig. 3 reports the experimental results of cyanate concentration vs. $E_{h\nu}$. It is notable that the nitrogen molar balance is closed only after the addition of hydrogen peroxide to the reacting system.

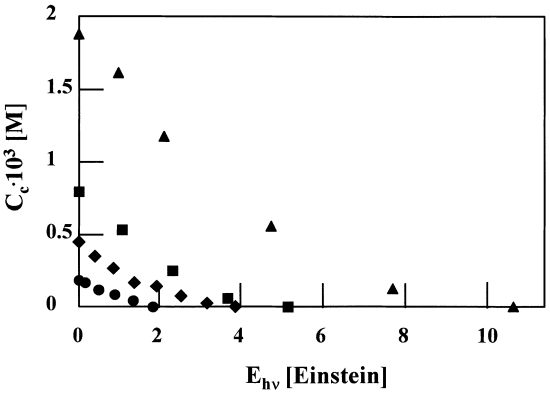

Fig. 4. Cyanide concentration versus cumulative photonic energy, $E_{h\nu}$, for runs carried out at the following initial cyanide concentrations: 0.18 mM (●); 0.45 mM (◆); 0.8 mM (■), and 1.87 mM (▲).

The influence of initial cyanide concentration on the degradation rate was also investigated. In Fig. 4, the measured values of cyanide concentration, C_C, are reported on a linear scale vs. $E_{h\nu}$ for typical runs carried

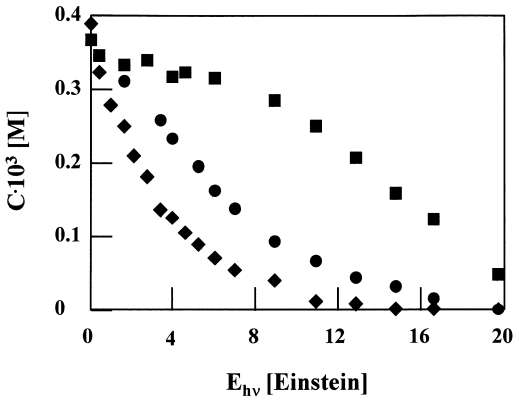

Fig. 5. Concentrations of cyanide (◆), phenol (●), and TOC (■) vs. cumulative photonic energy, $E_{h\nu}$.

out at different initial cyanide concentrations. From the observation of the data reported in Fig. 4, it can be noticed that a straight line fits the photoreactivity data for high values of cyanide concentration while an exponential line seems to fit the data for low values.

Some runs were carried out in the presence of phenol in order to study the influence of a model aromatic compound on the cyanide photo-oxidation reaction. Fig. 5 reports the values of cyanide, phenol and total organic carbon (TOC) concentrations vs. the cumulative photonic energy. It must be noted that the TOC values reported in Fig. 5 are equal to one sixth of the measured ones. Only in this way, in fact, is it possible to compare the TOC values with the phenol concentration values. The correctness of this procedure is justified by the finding that the main intermediate compounds found during phenol photo-oxidation are only aromatic compounds (catechol, quinone). The absence of detection of C_n aliphatic products with $n < 6$ suggests that the opening of aromatic ring produces compounds which remain adsorbed on the catalyst surface until their complete oxidation to CO_2 [16]. By comparing the reactivity results reported in Fig. 5 with those of Fig. 2, it may be noted that the presence of phenol negatively affects the cyanide photo-oxidation rate.

The reactivity test, carried out using CNO^- as substrate in the laboratory batch photoreactor, lasted 10 h. This run indicated that the cyanate photodegradation occurs at a low rate, as expected [7], and that nitrite and nitrate ions are produced together with traces of ammonia. The runs carried out using NH_2OH showed that this compound exhibits a negligible reactivity in the absence of radiation; at equal reaction conditions, but, in the presence of radiation, NH_2OH completely disappeared in <1 h by producing measurable quantities of ammonia, nitrite and nitrate ions.

4. Discussion

4.1. Mechanistic aspects

The CPC photoreactivity results, obtained in this work, indicate that cyanate ion is the first photo-oxidation product of cyanide; the subsequent cyanate photo-oxidation eventually determines the formation of nitrite and nitrate ions whose amounts, however, denote a lack of nitrogen mass balance in the course of the reaction. The addition of H_2O_2 to the reacting system determines the closure of nitrogen mass balance even if the photo-oxidation rate of CNO^- does not significantly change in the presence of H_2O_2.

In a photocatalytic process, the primary step following the absorption of radiation by the photocatalyst is the generation of electron–hole pairs which must be trapped in order to avoid recombination [2]. As a consequence of the trapping steps, several species are produced. The hydroxyl groups are likely traps for holes leading to the formation of hydroxyl radicals while the adsorbed oxygen species are traps for electrons.

Frank and Bard [3] and Augugliaro et al. [7] report that CNO^- is the first product of photocatalytic oxidation of cyanides in the presence of polycrystalline TiO_2 in aqueous medium. As far as the formation of isocyanate species is concerned, it is, in principle, possible. Indeed, the isocyanic acid is more stable than the cyanic one [17], but the two anion species in tautomeric equilibrium are predominant in a strongly alkaline medium. It is reasonable to hypothesise that this equilibrium is displaced towards the cyanate form due to the higher electronegativity of oxygen on respect to nitrogen. The proposed mechanism implies the oxidation of cyanide by the photogenerated holes and the reduction of oxygen by electrons according to the following overall equations:

$$CN^- + 2h^+ + 2OH^- \rightarrow CNO^- + H_2O \quad (3)$$

$$O_2 + 2e^- + 2H_2O \rightarrow H_2O_2 + 2OH^- \quad (4)$$

Augugliaro et al. [7] also report that cyanate ions are photo-oxidised to nitrates and a satisfactory nitrogen balance is achieved according to the following overall reaction:

$$CNO^- + 4O_2 + 2OH^- + 3H_2O \rightarrow CO_3^{2-} + NO_3^- + 4H_2O_2 \quad (5)$$

The absence of nitrogen mass balance, as found in this work in accord with the studies by Mihaylov et al. [6], or its occurrence, as also found in this work in accord with Augugliaro et al. [7], can be justified by considering the oxidative experimental conditions under which the cyanate photo-oxidation was carried out. The CPC operative conditions, such as the low values of incident photon flow and of oxygen concentration in the dispersion and the nature of the catalyst used, can determine mild oxidation conditions and, as a consequence, the formation of volatile nitrogen-containing species (such as NH_3, N_2, N_2O, etc.) together with that of nitrite and nitrate ions. At strong oxidant conditions, such as determined in the presence of large amounts of H_2O_2, volatile nitrogen-containing species are not produced or are quickly photo-oxidised to NO_2^- and NO_3^-.

It is useful to stress the point that, in this work, a satisfactory mass balance for nitrogen was achieved only when H_2O_2 was added to the reacting system. The cyanate photo-oxidation carried out in the laboratory photoreactor at mild oxidation conditions produced nitrite, nitrate, ammonia and/or volatile unidentified species. Ammonia was not detected when the runs were carried out by adding H_2O_2. The finding that the photo-oxidation rate of CNO^- does not significantly change in the presence of H_2O_2 suggests that the cyanate photo-oxidation occurs via a highly reactive intermediate species whose formation rate is not affected by H_2O_2. It is likely that this species is NH_2OH. It is well known, in fact, that the fate of NH_2OH is very complex [18]: it can disproportionate by producing reduced and oxidised nitrogen-containing species and/or it can be oxidised to volatile nitrogen containing species. On the basis of all the experimental results and of the previous considerations, the following reaction pathway can be hypothesised:

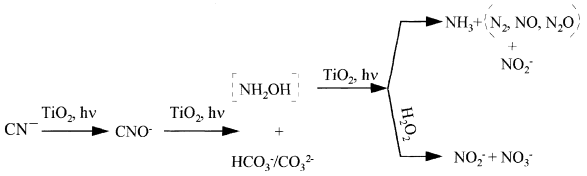

The selectivity among the various routes is obviously affected by the oxidant conditions of the reacting medium. Even if it was impossible to experimentally determine the presence of NH_2OH in the course of cyanide photodegradation, the reaction mechanism above proposed is able to explain the main indications of this work, i.e. the findings that:

1. the presence of NH_3, NO_2^- and NO_3^- is observed when the photocatalytic oxidation of CNO^- and NH_2OH is carried out at mild oxidation conditions, such as those prevailing in the laboratory photoreactor; and
2. only NO_2^- and NO_3^- are detected when the addition of H_2O_2 determines strong oxidant conditions.

4.2. Kinetic aspects

The following considerations can be drawn by all the photoreactivity results:

1. the cyanide photo-oxidation occurs according to zero order kinetics at high concentrations of cyanide;
2. the reaction turns to first order kinetics when the cyanide concentration decreases;
3. the cyanate photocatalytic oxidation only starts after the almost complete oxidation of cyanide ions;
4. the rate of cyanate photo-oxidation is smaller than that of cyanide: at equal reaction conditions the initial reaction rate of cyanide is about one order of magnitude higher than that of cyanate;
5. the phenol photo-oxidation exhibits the same features shown by the cyanide; and
6. the presence of phenol is detrimental for the photo-oxidation rate of cyanide.

The following chemical kinetic model is proposed for modelling the reactivity results. The rate determining step for the photo-oxidation process is hypothesised to be the reaction between OH radicals and cyanide ions on the catalyst surface. The concentration of OH radicals depends on the fractional sites cover-

age by O_2 due to the fact that oxygen acts as an electron trap, thus hindering the electron–hole recombination. Two different types of active sites are hypothesised to exist over the catalyst surface. The first ones are able to photoadsorb cyanide ions and the others are able to photoadsorb oxygen. The reaction rate for the second-order surface oxidation of cyanide may be written in terms of Langmuir–Hinshelwood kinetics as:

$$r = -\frac{dC_c}{dt} \equiv k''\theta_o\theta_c \tag{6}$$

in which C_c is the cyanide concentration, t the irradiation time, k'' the surface second-order rate constant and θ_o and θ_c the fractional sites coverage by oxygen and cyanide, respectively. k'' depends on the radiation intensity, I, according to the following power law, $k'' = kI^{\alpha}$, α being a coefficient in the 0.5–1 range [19]. The results obtained at different irradiances indicate that, in the present case, $\alpha = 1$. The fractional site coverages by cyanide ions and by oxygen are given by the following relationships:

$$\theta_c = \frac{K_c C_c}{1 + K_c C_c} \tag{7}$$

$$\theta_{oxygen} = \frac{K_o C_o}{1 + K_o C_o} \tag{8}$$

in which K_c and K_o are the equilibrium photoadsorption constants for cyanide and oxygen, respectively, and C_o the oxygen concentration in the aqueous phase. Owing to the fact that the dispersion was continuously in contact with atmospheric air, it can be assumed that for all the runs θ_o is constant during the occurrence of cyanide photo-oxidation. On the basis of all the previous statements, Eq. (6) can be written as:

$$r = -\frac{dC_c}{dt} \equiv \frac{k'_c I K_c C_c}{1 + K_c C_c} \tag{9}$$

in which k'_C is the surface pseudo-first order rate constant and it is equal to $k''\theta_o$.

The photoreacting system used in this work (see Fig. 1) is composed by a PFP and a SNT. The irradiated PFP determines the occurrence of cyanide degradation while the SNT determines that the cyanide concentration at the PFP inlet, $C_{C,out}$, is different from the outlet one, $C_{C,in}$. The system is not at steady state so that the PFP inlet and outlet concentrations are varying with time. The cyanide mass balance equations modelling the PFP and SNT behaviour are:

$$\text{(PFP)} \qquad \frac{dC_c}{dt} = -W\frac{dC_c}{dV} - Z \tag{10}$$

$$\text{(SNT)} \qquad \frac{dC_{c,out}}{dt} = \frac{W}{V_{SNT}}(C_{c,in} - C_{c,out}) \tag{11}$$

in which W is the volumetric flow rate, C_c the cyanide concentration in a volume, dV, belonging to the PFP (C is a function of time and of axial position in the photoreactor), and V_{SNT} the liquid volume inside the stirred tank.

The dynamics of this photoreacting system has been discussed in detail by Wolfrum and Turchi [20] for a photocatalytic reaction whose kinetics obeys the Langmuir–Hinshelwood rate expression reported in Eq. (9). At high values of C_c ($K_c C_c \gg 1$) and at low values of C_c ($K_c C_c \ll 1$) the rate equation approaches zero order and first order, respectively. The authors [20] analyse these two limiting situations and demonstrate that, in both the cases, provided that the value of the photoreactor residence time is small, the following relationship holds:

$$-\frac{dC_{c,out}}{dt} = \frac{V_{PFP}}{V_T} r(C_{c,out}) \tag{12}$$

in which $r(C_{c,out})$ is the rate equation evaluated at $C_c = C_{c,out}$. In other words, in a recycle system with low per-pass conversion determined by low values of residence time for zero and first order kinetics, the observed reactivity data must be normalised by multiplying them by the ratio of the photoreactor volume to the total volume, V_{PFP}/V_T in the present case.

The assumption is made here that Eq. (12) holds also for reaction order in the 0–1 range, i.e. also for the Langmuir–Hinshelwood rate expression:

$$-\frac{dC_{c,out}}{dt} = \frac{V_{PFP}}{V_T}\frac{k'_C I K_c C_{c,out}}{1 + K_c C_{c,out}} \tag{13}$$

Eq. (13) can be written as:

$$-\frac{dC_{c,out}}{d(E'_{h\nu})} = \frac{k'_C K_c C_{c,out}}{1 + K_c C_{c,out}} \tag{14}$$

In which $E'_{h\nu} = I t V_{PFP}/V_T$. By assuming that the photoreactor performance during the first residence time negligibly affects the photoreactivity results, Eq. (14) can be easily integrated with the limiting condition

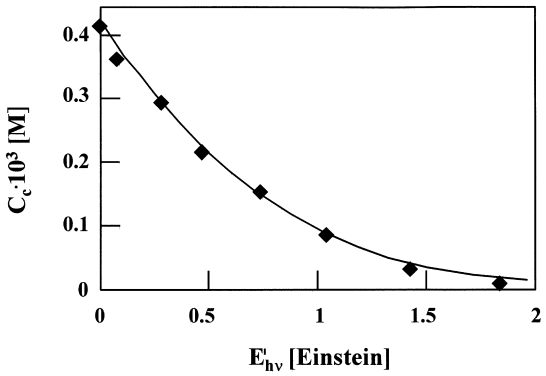

Fig. 6. Cyanide concentrations vs. cumulative photonic energy, $E_{h\nu}$. Comparison between the experimental data (◆) and the kinetic model expressed by Eq. (15) (—).

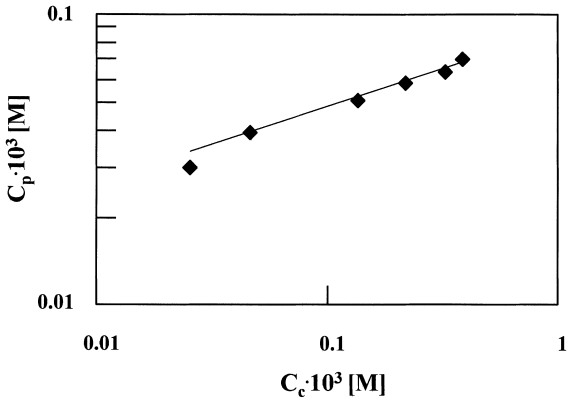

Fig. 7. Phenol concentration versus cyanide concentration. Comparison between the experimental data (◆) and the kinetic model expressed by Eq. (18) (—).

that for $E'_{h\nu} = 0$, the cyanide-ion concentration is equal to the initial one, $C_{c,out} = C_0$. The integral relationship between $C_{c,out}$ and $E'_{h\nu}$ is therefore:

$$E'_{h\nu} = \frac{1}{A}\ln\left(\frac{C_0}{C_{c,out}}\right) + \frac{1}{B}(C_0 - C_{c,out}) \quad (15)$$

where $A = k'_c K_c$ and $B = k'_c$. By applying a least-squares best fitting procedure to the photoreactivity data obtained from cyanide degradation, the values of A and B can be determined. The values of k'_c and K_c are 10^{-3} M/Einstein and 2700 M^{-1}, respectively. In Fig. 6, the line through the experimental data of cyanide concentration has been drawn by using Eq. (15); it may be noticed that a satisfactory fitting of the model to the data occurs. The phenol reactivity data have been treated with the above reported kinetic model. For phenol the values of the surface pseudo-first-order rate constant, k'_p, and of equilibrium photo-adsorption constant, K_P, are 0.14×10^{-3} M/Einstein and 6500 M^{-1}, respectively.

When both phenol and cyanide are present in the reacting medium, it is reasonable to hypothesise a competitive photoadsorption mechanism on the same active sites. The Langmuir–Hinshelwood kinetic equations for cyanide and phenol degradation are:

$$-\frac{dC_c}{dt} = \frac{k'_c I K_c C_c}{1 + K_c C_c + K_p C_p} \quad (16)$$

$$-\frac{dC_p}{dt} = \frac{k'_p I K_p C_p}{1 + K_c C_c + K_p C_p} \quad (17)$$

where C, k', K indicate concentration, surface pseudo-first order kinetic constant and equilibrium photo-adsorption constant while the subscripts c and p refer to cyanide and phenol, respectively. On dividing Eq. (17) by Eq. (16), and rearranging, the differential equation relating C_p and C_c at whatever time is obtained. The integration of this first-order differential equation with the limiting condition that $C_p = C_{p,0}$ for $C_c = C_{c,0}$, where $C_{p,0}$ and $C_{c,0}$ represent the initial concentrations of phenol and cyanide, respectively, gives the following relationship:

$$\ln\frac{C_p}{C_{p,0}} = \frac{k'_p K_p}{k'_c K_c}\ln\frac{C_c}{C_{c,0}} \quad (18)$$

By applying a least-squares best fitting procedure to the experimental data, the values of the group $(k'_p K_p)/(k'_c K_c)$ were determined for all the runs carried out at different molar ratios between cyanide and phenol. These values were in the 0.30–0.38 range and did not show a dependence on the cyanide/phenol ratio. In Fig. 7, a logarithmic diagram reports experimental results of phenol concentration versus cyanide concentration. It may be noted that a straight line, whose slope represents the $(k'_p K_p)/(k'_c K_c)$ quantity, well fits the data.

The value of the $(k'_p K_c)/(k'_p K_c)$ group, calculated from the k' and K figures determined for cyanide and phenol separately, was 0.33. This value is quite similar to those previously reported so that it may be concluded that the competitive photo-adsorption mecha-

nism well describes the reactivity results. It is worth noting, finally, that the model described above is only a phenomenological one and it cannot be invoked for proving mechanistic aspects of the photoprocess.

5. Conclusions

The results of this work indicate that the heterogeneous photocatalytic method can be successfully used for eliminating cyanide ions from wastewater by using the sun as radiation source. The free cyanide oxidation has been carried out in aqueous suspensions containing polycrystalline TiO_2 irradiated by sunlight. Under the experimental conditions, the photoreaction proceeds at a measurable rate until the complete disappearance of cyanide ions. The main oxidation products of cyanide ions are cyanate, nitrite, nitrate and carbonate ions. At mild oxidation conditions of the photoprocess the nitrogen mass balance, carried out on the dissolved compounds, is not satisfied in the course of cyanate photo-oxidation, thus indicating the formation of some volatile species. The nitrogen mass balance is, however, closed at strong oxidation conditions determined by the addition of H_2O_2 to the solution. The efficiency of cyanide oxidation process decreases in the presence of a competitive oxidation reaction regarding an organic compound (phenol) present in the reacting medium. The kinetic model of Langmuir–Hinshelwood well describes the photoreactivity results obtained with cyanide and cyanide-phenol solutions.

Acknowledgements

The authors wish to thank the ‘Innovative Training Horizons in Applied Solar Thermal and Chemical Technologies’ (contract ERBMFGE-CT95-0023 of the EEC Training and Mobility of Researchers Program) for financial support and availability of the facilities located at the Plataforma Solar of Almería (Spain).

References

[1] D.F. Ollis, H. Al-Ekabi (Eds.), Photocatalytic Purification and Treatment of Water and Air, Elsevier, Amsterdam, 1993.
[2] M. Schiavello (Ed.), Photocatalysis and Environment, Trends and Applications, Kluwer, Dordrecht, 1988.
[3] S.N. Frank, A.J. Bard, J. Am. Chem. Soc. 99 (1977) 303.
[4] J. Peral, X. Doménech, J. Photochem. Photobiol. A: Chem. 53 (1992) 93.
[5] H. Hidaka, T. Nakamura, A. Ishizaka, M. Tsuchiya, J. Zhao, J. Photochem. Photobiol. A: Chem. 66 (1992) 367.
[6] B.V. Mihaylov, J.L. Hendrix, J.H. Nelson, J. Photochem. Photobiol. A: Chem. 72 (1993) 173.
[7] V. Augugliaro, V. Loddo, G. Marcì, L. Palmisano, M.J. López Muñoz, J. Catal. 166 (1997) 272.
[8] S.Q. Hassan, M.P. Kupfeleand, D.W. Grosse, J. Air Waste Manage. Assoc. 41 (1991) 710.
[9] D.W. Grosse, J. Air Pollution Control Assoc. 36 (1986) 603.
[10] M. Futakawa, H. Takahashi, G. Inoue, T. Fujioka, Desal. 98 (1994) 345.
[11] L.P. Salomonson, in B. Vennesland, E.E. Conn, C.J. Knowles, J. Westley, F. Wissing (Eds.), Cyanide in Biology, Academic Press, New York, 1981.
[12] S. Malato Rodríguez, C. Richter, J. Blanco Gálvez, M. Vincent, Solar Energy 56 (1996) 401.
[13] S. Malato, J. Blanco, C. Richter, D. Curcò, J. Jiménez, Wat. Sci. Tech. 35 (1997) 157.
[14] J.M. Herrmann, J. Disdier, P. Pichat, S. Malato, J. Blanco, Appl. Catal. B: Environ. 17 (1998) 15.
[15] A.E. Greenberg, L.S. Clesceqi, A.D. Eaton (Eds.), Standard Methods for the Examination of Water and Wastewater, American Public Health Association, Washington DC, 1992.
[16] V. Augugliaro, L. Palmisano, A. Sclafani, C. Minero, E. Pelizzetti, Toxicol. Environ. Chem. 16 (1988) 89.
[17] J.C. Bailar, H.J. Emeléus, R. Nyholm, A.F. Trotman-Dickenson (Eds.), Comprehensive Inorganic Chemistry, vol. 1, Pergamon Press, Oxford 1973, p. 1247.
[18] J.C. Bailar, H.J. Emeléus, R. Nyholm, A.F. Trotman-Dickenson (Eds.), Comprehensive Inorganic Chemistry, vol. 3, Pergamon Press, Oxford 1973, p. 265.
[19] P. Pichat, in: M. Schiavello (Ed.), Photoelectrochemistry, Photocatalysis and Photoreactors. Fundamentals and Developments, Reidel, Dordrecht 1985, p. 425.
[20] E.J. Wolfrum, C.G. Turchi, J. Catal. 136 (1992) 626.